新疆西昆仑造山带北缘中元古代帕什托克闪长岩侵入序列及其地质意义

赵佳楠[1,2] 刘正军[3]

（1.中国地质大学（北京）地球科学与资源学院，北京 100083；2.中国地质科学院地质研究所，大陆构造与动力学国家重点实验室，北京 100037；3.湖南省地质科学研究院，湖南 长沙 410007）

提要：位于塔里木地块西南缘、西昆仑造山带北缘的帕什托克侵入序列由石英闪长岩-石英二长闪长岩组成，类似TTG组合，形成于中元古代晚期。本文从帕什托克侵入序列的地球化学分析出发，通过对该侵入序列两期侵入岩的主量元素和微量元素的研究，讨论了该侵入序列的成因、构造环境和与其相关的板块间地球动力学模式，认为该侵入序列为I型准铝质高钾钙碱性花岗闪长岩系列，属活动板块边缘碰撞前大陆弧花岗岩类，两期侵入岩为同源岩浆演化，母岩浆属壳幔混合源，且岩浆向酸性演化。根据岩浆演化的物理环境和构造环境，推测早古生代库地洋的完全闭合与库地洋壳向塔里木古陆块俯冲消减有关，是塔里木古陆块和柴达木古陆块在Rodinia超级大陆汇聚过程中的产物。

关 键 词：西昆仑造山带；帕什托克闪长岩侵入序列；地球化学；构造环境；地球动力学

中图分类号：P588.122 **文献标志码**：A **文章编号**：1000-3657(2014)01-0092-16

毗邻塔里木地块西南缘的西昆仑造山带，是中国古亚洲构造域与古特提斯构造域的缝合带[1-8]。塔里木古板块曾被认为是Rodinia超级大陆的一部分[1-5]。在西昆仑造山带北缘出露的前寒武纪岛弧活动带花岗岩主要为I型花岗岩，可能属幔源同熔成因，并存在地壳物质部分熔融，很可能形成于碰撞前汇聚消减板块边缘环境，与洋壳俯冲密切相关[6-12]，其成因和构造背景以及与Rodinia超大陆之间的关系值得深入研究。本文以塔里木地块西南部中元古代帕什托克中酸性岩侵入序列作为研究对象，对该侵入序列主量和微量元素进行详细分析，讨论了该侵入序列的成因和构造环境，并探讨了帕什托克侵入序列的演化和地球动力学背景，为探究中元古代大地构造格局提供可靠的研究资料，且对塔里木地块的地球动力学研究具重要意义。

1 地质背景

西昆仑造山带位于塔里木地块的西南部、羌塘地块的东北部，处在塔什库尔干断裂以东、阿尔金断裂西南部以西，被乌塔格—库尔勒断裂和康西瓦断裂分割成3个次级构造带，分别为西昆仑北构造带、西昆仑南构造带和喀喇昆仑构造带[7-13]，其中在西昆仑南、北两构造带中广泛分布中元古代地层和岩浆岩（图1）。

研究区位于羌塘地块和塔里木地块之间的西昆仑中间地块，地理坐标为：E76°15′~76°30′，N37°30′~37°50′。中元古代，研究区两侧分别发育喀喇昆仑洋和库地洋，北侧库地洋至早古生代完全闭合，

收稿日期：2013-03-20；**改回日期**：2013-10-27

基金项目：国家自然科学基金委创新群体项目（40921001）和国家自然科学基金项目（40702036）联合资助。

作者简介：赵佳楠，男，1989年生，博士生，主要从事大地构造及构造地质学、油气储层和遥感地质找矿研究；E-mail：zhaojianan1989@163.com。

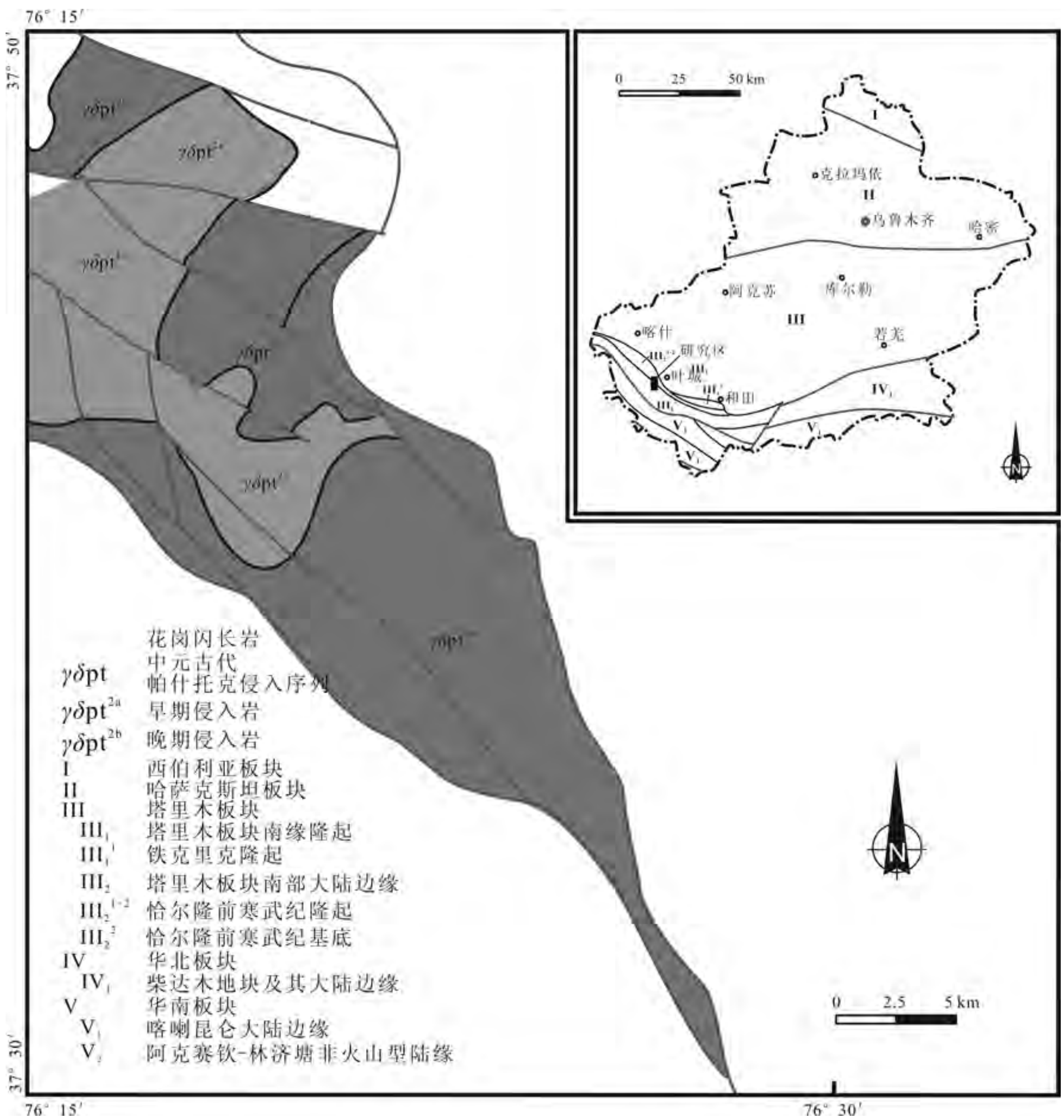

图1 研究区区域大地构造略图和帕什托克侵入序列空间展布
Fig.1 Simplified regional tectonic map of the study area and spatial distribution map of Pashtok intrusive sequence

南侧喀喇昆仑洋至中生代晚期闭合,形成康西瓦缝合带[13]。帕什托克岩体于中元古代侵入,岩体面积为200.56 km^2,占整个研究区面积的40.06%,Sm–Nd同位素年龄为(1200±82) Ma[2–4,14]。帕什托克侵入序列主要由花岗闪长岩–石英二长闪长岩组成,类似TTG组合,侵入岩体空间展布方向为近NW–SE向。该侵入序列分两个侵入期次,早期为中粗粒石英二长闪长岩–石英闪长岩,晚期为中细粒花岗闪长岩–英云闪长岩,均具半自形粒状结构,块状构造,二者接触界线不明显,呈隐蔽式侵入接触,晚期侵入的花岗闪长岩–英云闪长岩与早期石英二长闪长岩–石英闪长岩之间存在宽度不等的同化混染带,宽者可达20 cm。

2 岩石化学

对帕什托克侵入序列中10件具代表性的岩石样品进行地球化学分析(表1),早期侵入岩(XJ11–G02、XJ11–G05、XJ11–G06、XJ11–G10)的SiO_2平均

表1 帕什托克侵入序列主量元素(%)、CIPW标准矿物(%)及其特征参数

Table 1 Chemical compositions of major elements (%), CIPW standard mineral (%), and characteristic parameters of Pashtok intrusive sequence

分析项目	XJ11-G01	XJ11-G02	XJ11-G03	XJ11-G04	XJ11-G05	XJ11-G06	XJ11-G07	XJ11-G08	XJ11-G09	XJ11-G10
SiO_2	57.15	55.99	58.08	58.11	54.95	56.96	58.72	57.66	59.34	57.44
TiO_2	0.66	0.68	0.54	0.65	0.71	0.67	0.62	0.68	0.62	0.65
Al_2O_3	16.03	15.74	15.99	16.75	17.67	16.87	16.34	16.68	16.31	16.49
Fe_2O_3	3.42	1.91	2.24	1.92	1.81	1.92	1.77	1.65	1.67	2.03
FeO	3.42	4.69	4.32	4.79	5.48	4.90	4.73	5.20	4.63	4.68
MnO	0.13	0.14	0.15	0.11	0.10	0.12	0.10	0.10	0.11	0.12
MgO	3.20	2.99	2.55	2.87	2.93	2.92	2.78	2.90	2.48	2.85
CaO	6.10	6.35	5.83	5.54	6.53	6.05	4.97	5.88	5.54	5.87
Na_2O	2.65	3.03	2.62	2.56	2.67	3.21	2.62	2.69	2.58	2.74
K_2O	3.10	3.43	3.16	3.05	3.13	2.64	3.49	2.85	3.37	3.14
P_2O_5	0.12	0.18	0.18	0.19	0.21	0.18	0.15	0.15	0.16	0.16
LOI	3.42	5.25	3.88	4.79	4.22	4.56	4.36	4.48	4.41	4.34
Total	99.39	100.39	99.54	101.33	100.42	101.01	100.66	100.91	101.24	100.50
石英(Q)	12.06	7.60	14.17	13.74	7.36	9.79	13.58	12.43	14.64	11.83
钙长石(An)	23.65	20.16	23.52	26.09	28.04	24.67	23.37	25.95	23.72	24.36
钠长石(Ab)	23.38	26.98	23.21	22.43	23.48	28.20	23.06	23.59	22.54	24.09
正长石(Or)	19.14	21.33	19.55	18.70	19.26	16.20	21.41	17.46	20.60	19.29
透辉石(Di)	5.82	9.64	4.55	0.91	3.47	4.35	0.98	2.70	2.98	3.95
紫苏辉石(Hy)	10.64	9.59	10.11	13.51	13.77	12.17	13.34	13.68	11.43	11.74
钛铁矿(Il)	1.31	1.36	1.08	1.28	1.40	1.32	1.22	1.34	1.22	1.28
磁铁矿(Mt)	3.74	2.91	3.39	2.89	2.72	2.89	2.67	2.48	2.50	3.07
磷灰石(Ap)	0.28	0.44	0.43	0.46	0.51	0.43	0.37	0.37	0.38	0.40
合计	100.02	100.01	100.01	100.01	100.00	100.01	100.00	100.00	100.01	100.01
全碱(ALK)	5.75	6.47	5.79	5.61	5.80	5.86	6.11	5.54	5.95	5.88
A/CNK	0.85	0.78	0.87	0.95	0.90	0.88	0.95	0.92	0.91	0.89
里特曼指数(δ)	2.34	3.22	2.22	2.09	2.82	2.46	2.38	2.09	2.17	2.39
分异指数(*DI*)	54.58	55.91	56.93	54.87	50.1	54.19	58.05	53.48	57.78	55.21
固结指数(*SI*)	20.38	18.64	17.15	18.89	18.31	18.71	18.06	18.99	16.85	18.45
碱度率(*AR*)	1.70	1.83	1.72	1.67	1.63	1.69	1.80	1.65	1.75	1.71
R_1	2026	1738	2098	2123	1833	1900	2047	2090	2128	1998
R_2	1175	1195	1113	1102	1238	1165	1028	1141	1070	1136
A/MF	0.93	0.94	1.04	1.01	1.01	1.00	1.02	0.99	1.09	1.00
C/MF	0.64	0.69	0.69	0.61	0.68	0.66	0.56	0.63	0.67	0.65

注：ALK=Na_2O+K_2O; A/CNK=$Al_2O_3/(CaO+Na_2O+K_2O)$; A/NK=$Al_2O_3/(Na_2O+K_2O)$; 里特曼指数$\delta=(K_2O+Na_2O)^2/(SiO_2-43)$; R_1=4Si-11(Na+K)−2(Fe+Ti); R_2=6Ca+2Mg+Al; A/MF=Al_2O_3/(TFeO+MgO)(mol); C/MF=CaO/(TFeO+MgO)(mol)。

含量为56.3%，Al_2O_3平均含量为16.7%，Fe_2O_3平均含量为1.9%，FeO平均含量为4.9 %，CaO平均含量为6.2%，K_2O平均含量为3.1%，P_2O_5平均含量为0.18%，通过QAP分类图解(图2–a)得出其主要为石英二长闪长岩，少量为石英闪长岩。全碱(ALK)平均值约为6.0，里特曼指数δ平均值为2.7(<3.3)，反映早期侵入岩属钙碱性岩，通过A/NK–A/CNK图解(图2–c)、SiO_2–AR图解(图2–d)和K_2O–SiO_2图解(图2–e)分析表明早期侵入岩为准铝质高钾钙碱性岩，与黎彤(1963)[15]中性岩、闪长岩和石英闪长岩平均值相比，具高Fe^{2+}低Fe^{3+}、高Ca高K低P的特征。晚期侵入岩的SiO_2平均含量为58.2%，FeO平均含量为4.5%，CaO平均含量为5.6%，K_2O平均含量为3.2%，P_2O_5平均含量为0.16%，QAP分类图解(图2–a)显示晚期侵入岩主要为花岗闪长岩，少为英云闪长岩。对比黎彤(1963)[15]花岗闪长岩、酸性岩和中性岩平均含量，晚期侵入岩保留了中性岩高铁镁高钙的特征，并具有酸性岩高K低P的特征。K_2O–SiO_2图解(图2–e)、A/NK–A/CNK图解(图2–c)和SiO_2–AR图解(图2–d)表明晚期侵入岩也与早期侵入相一样属准铝质高钾钙碱性岩。通过CIPW标准矿物计算和An–Ab–Or分类图解(图2–b)，帕什托克侵入序列属花岗闪长岩系列，说明该侵入序列由中性岩向酸性岩演化。

帕什托克侵入序列的A/CNK平均为0.89(<1)，A/NK=2.09，反映该序列为准铝质花岗岩(图2–c)，Na_2O含量为2.6%~3.2%，平均含量为2.8%(>2.2%)，早期和晚期侵入岩的Na_2O和K_2O平均值分别为2.9%和3.1%、2.6%和3.2%，表明早期侵入岩富Na，晚期侵入岩富K，且Na_2O/K_2O有减小趋势，CIPW标准矿物中含透辉石，符合I型花岗岩特征[15–16]。

3　地球化学

3.1 稀土元素

帕什托克侵入序列稀土元素总含量平均为170×10^{-6}，LREE/HREE平均为9.33(表2)，$(La/Yb)_N$平均值为10.4，$(La/Sm)_N$平均值为4.4，$(Gd/Lu)_N$平均值为1.5，反映该序列轻稀土元素和重稀土元素分馏明显，侵入序列富集轻稀土元素而亏损重稀土元素，且轻稀土元素分馏程度高，重稀土元素分馏程度低，呈现左陡峭右平滑的右倾型稀土元素配分曲线(图3–a)。该序列δEu平均为0.76，δCe平均为0.97，表明侵入序列Eu呈较明显负异常，Ce异常不明显，可视为无异常，与I型花岗岩稀土元素特征相似[22–24]，反映帕什托克侵入序列有可能属壳幔混合源。

帕什托克早期侵入岩与晚期侵入岩的稀土元素特征关系密切，早晚两期侵入岩总稀土元素范围分别为165×10^{-6}~174×10^{-6}和163×10^{-6}~197×10^{-6}，其中轻稀土元素总量平均值分别为152×10^{-6}和155×10^{-6}，LREE/HREE比值分别为9.21和9.41，反映帕什托克侵入序列属同源岩浆演化，演化晚期轻稀土元素富集，且该侵入序列酸性程度增加，具中性岩向酸性岩演化趋势。两期侵入岩$(Ce/Yb)_N$平均值分别为7.76和7.85，$(La/Sm)_N$平均值分别为4.44和4.34，$(Gd/Lu)_N$分别为1.50和1.45，δEu平均值分别为0.79和0.74，δCe平均值分别为0.95和0.98，表明该序列属同源岩浆演化，Eu负异常的增加与岩浆分离结晶作用有关，斜长石对Eu的分配系数远大于REE，分离结晶作用增强，斜长石的大量晶出控制着Eu在残余岩浆中亏损愈加明显，且Eu负异常的降低指示岩浆向酸性演化，与帕什托克侵入序列演化一致，而轻稀土和重稀土分异程度略微降低，Ce异常趋于1，反映地幔岩浆结晶分异过程中可能存在壳源物质混入，发生壳幔间同化混染。

3.2 微量元素

帕什托克侵入序列强烈富集Rb、Th，亏损Sr(图3–b，表2)，比较原始地幔和地壳标准化配分曲线，该侵入序列除存在地幔演化特征外，还存在与地壳微量元素特征类似的元素配分(图3–c)，指示该序列可能属壳幔混合源的同源演化，幔源物质结晶分异过程中同化混染了壳源物质。Rb–Sr图(图3–d)和Hf–Zr图(图3–e)显示，Sr与Rb、Hf与Zr存在线性相关，相关系数均为1，Sr与Rb为负相关，且存在高Sr低Rb向低Sr高Rb的演化趋势，而Hf与Zr为正相关，向高Hf高Zr演化，Rb/Sr–Zr/Hf图(图3–f)反映Zr/Hf与Rb/Sr呈负相关，二次拟合相关系数为0.99。表明帕什托克侵入序列属同源岩浆演化，在岩浆结晶分异过程中可能存在同化混染作用。Sr、Cr逐渐亏损，Rb、Th大量富集，指示该侵入序列向酸性岩系列演化。Nb、Ta也随着岩浆演化过程逐渐

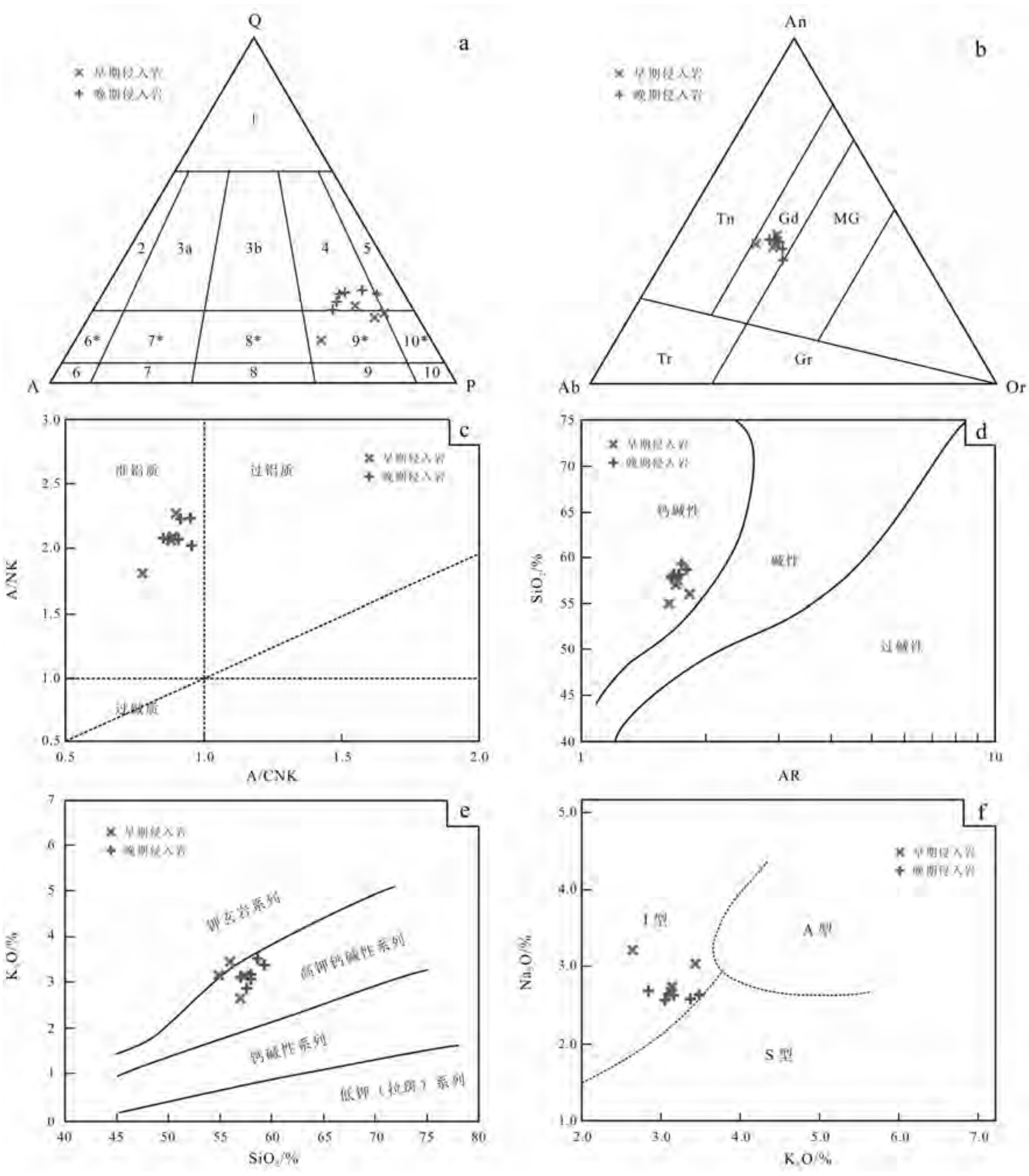

图2 帕什托克侵入序列岩石分类图解

a—花岗岩QAP分类图解[15]；1—富石英花岗岩；2—碱长花岗岩；3a—花岗岩；3b—花岗岩（二长花岗岩）；4—花岗闪长岩；5—英云闪长岩、斜长花岗岩；6—碱长正长岩；7—正长岩；8—二长岩；9—二长闪长岩；10—闪长岩、斜长岩；6*—碱长石英正长岩；7*—石英正长岩；8*—石英二长岩；9*—石英二长闪长岩；10*—石英闪长岩；b—花岗岩An—Ab—Or图解[16]；Tn—英云闪长岩；Gd—花岗闪长岩；MG—石英二长岩；Tr—奥长花岗岩；Gr—花岗岩；c—A/NK—A/CNK图解[17]； d—SiO_2—AR图解；e—K_2O—SiO_2图解[18]；f—Na_2O—K_2O花岗岩I−A−S分类图解[19]

Fig.2 Various classification diagrams of Pashtok intrusive sequence

a−QAP diagram of the Pashtok intrusive sequence[15]; 1−Quartz−rich granite; 2−Alkali−feldspar granite; 3a−Granite; 3b−Granite(monzogranite); 4−Granodiorite; 5−Tonalite; 6−Alkali−feldspar syenite; 7−Syenite; 8−Monzonite; 9−Monzonite diorite; 10−Diorit, plagioclasite; 6*−Alkali−feldspar quartz syenite; 7*−Quartz syenite; 8*−Quartz monzonite; 9*−Quartz monzonite diorite; 10*−Quartz diorite; b−An−Ab−Or diagram of the Pashtok intrusive sequence[16]; Tn−Tonalite; Gd−Granodiorite; MG−Quartz monzonite; Tr−Trondjemite; Gr−Granite; c−A/CNK−A/CK plot of the Pashtok intrusive sequence[17]; d−SiO_2−AR diagram of the Pashtok intrusive sequence; e−K_2O−SiO_2 diagram of the Pashtok intrusive sequence[18]; f−Na_2O−K_2O diagram of the Pashtok intrusive sequence[19]

表2 帕什托克侵入序列微量元素(10^{-6})及其特征参数

Table 2 Trace elements (10^{-6}) and characteristic parameters of Pashtok intrusive sequence

分析项目	XJ11-G01	XJ11-G02	XJ11-G03	XJ11-G04	XJ11-G05	XJ11-G06	XJ11-G07	XJ11-G08	XJ11-G09	XJ11-G10
Y	23.8	23.7	23.6	23.7	23.6	23.7	22.3	23.8	23.7	23.3
Rb	215	121	154	161	149	159	147	139	192	180
Sr	58.5	170.0	134.0	123	137	125	139	149	86	100
Zr	228	216	220	221	220	221	219	218	225	223
Nb	44.0	11.9	23.2	25.6	21.6	24.9	20.8	18.1	36.0	32.0
Th	91.3	8.88	37.7	43.9	33.6	41.9	31.6	24.7	70.7	60.4
Cr	7.92	22.0	17.1	16.0	17.8	16.3	18.1	19.3	11.4	13.2
Hf	6.64	5.62	5.98	6.05	5.93	6.03	5.90	5.82	6.39	6.26
Sc	4.02	19.6	14.1	13.0	14.9	13.3	15.3	16.6	7.91	9.85
Ta	3.09	0.80	1.60	1.77	1.49	1.72	1.43	1.24	2.52	2.23
Co	0.05	0.02	0.03	0.03	0.03	0.03	0.03	0.03	0.04	0.04
B	2.60	5.80	4.68	4.44	4.84	4.52	4.92	5.19	3.40	3.80
La	30.2	36.6	34.2	39.0	36.3	35.8	44.7	36.2	34.6	37.8
Ce	65.1	68.4	68.6	76.0	69.7	68.7	84.4	71.3	67.7	73.1
Pr	7.63	8.08	8.00	8.78	8.15	8.04	9.57	8.31	7.93	8.45
Nd	30.1	30.6	30.4	32.0	30.5	29.1	35.4	31.1	29.7	31.3
Sm	4.90	5.10	5.20	5.90	5.27	5.45	5.80	5.45	5.23	5.48
Eu	1.13	1.38	1.23	1.35	1.31	1.30	1.28	1.31	1.28	1.29
Gd	4.48	4.63	4.66	5.20	4.71	4.86	4.74	4.87	4.71	4.79
Tb	0.71	0.79	0.74	0.77	0.76	0.75	0.74	0.76	0.75	0.75
Dy	4.13	4.38	4.22	4.42	4.30	4.29	4.16	4.33	4.27	4.26
Ho	0.82	0.85	0.84	0.87	0.85	0.87	0.84	0.85	0.85	0.85
Er	2.53	2.58	2.52	2.58	2.53	2.50	2.40	2.57	2.53	2.50
Tm	0.41	0.40	0.39	0.40	0.39	0.37	0.38	0.40	0.39	0.38
Yb	2.68	2.63	2.56	2.55	2.54	2.39	2.44	2.60	2.52	2.48
Lu	0.45	0.40	0.41	0.40	0.40	0.37	0.38	0.41	0.40	0.39
ΣREE	155	166	163	180	168	165	197	171	163	174
LREE	139	150	148	163	151	148	181	154	146	157
HREE	16.2	16.6	16.3	17.2	16.5	16.4	16.1	16.8	16.4	16.4
LREE/HREE	8.59	9.02	9.04	9.48	9.18	9.05	11.3	9.15	8.93	9.59
La_N/Yb_N	8.10	10.0	9.58	11.0	10.3	10.8	13.1	9.99	9.85	10.9
δEu	0.72	0.85	0.75	0.73	0.79	0.76	0.72	0.76	0.77	0.75
δCe	1.02	0.93	0.98	0.97	0.95	0.95	0.95	0.97	0.97	0.96

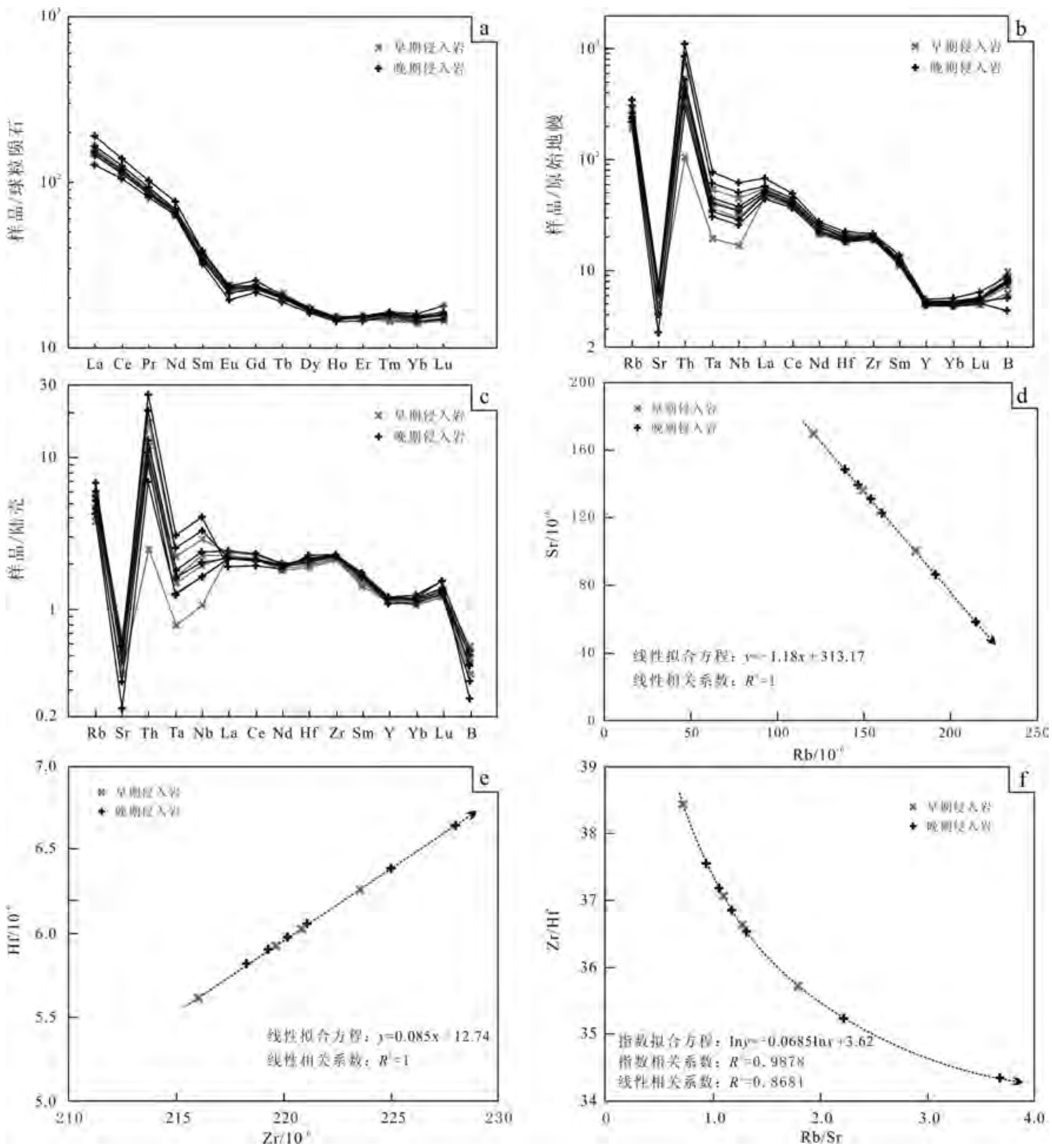

图3 稀土元素和微量元素分析图解

a—帕什托克侵入序列稀土元素球粒陨石标准化配分曲线[28]；b—微量元素标准化配分曲线[28]；c—微量元素标准化配分曲线[28]；d—Rb−Sr图；e—Zr−Hf图；f—Rb/Sr−Zr/Hf图

Fig.3 Analytical diagrams of REE and trace elements for Pashtok intrusive sequence

a−Chondrite−normalized REE patterns[28]; b−Primitive−mantle−normalized spidergrams[28]; c− Primitive−crust−normalized spidergrams[28]; d−Rb−Sr diagram; e−Zr−Hf diagram; f−Rb/Sr−Zr/Hf diagram

富集，反映该序列存在矿化[23]。

4 讨论

4.1 成因类型

通过对帕什托克侵入序列主量元素和微量元素分析，表明帕什托克侵入序列与I型花岗岩特征类似，QAP图解（图4）显示帕什托克侵入序列属I型钙碱性花岗闪长岩（中钾）系列。磷灰石在岩浆分异过程中的行为也被用来区分成因类型，在岩浆分异过程中，准铝质岩浆中的磷灰石溶解度极低，且

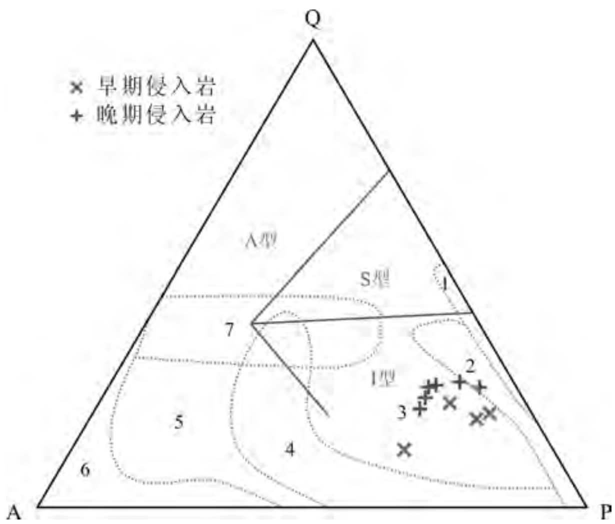

图4 QAP成因分类图解[29]
1—拉斑玄武岩系列的花岗岩;2—钙碱性奥长花岗岩(低钾)系列;3—钙碱性花岗闪长岩(中钾)系列;4—二长岩(高钾)系列;5—碱性岩石的铝质花岗岩系列;6—碱性及过碱性系列;7—地壳熔融生成的花岗岩类岩石

Fig.4 QAP genetic classification diagram[29]
1−Tholeiite series of granite; 2− Calc−alkaline trondhjemite (low K) series; 3−Calc−alkaline granodiorite (intermediate K) series; 4−Monzonites (high potassium) series; 5−Peraluminous granites series of alkaline rocks; 6−Alkaline and peralkaline series; 7−Granitoids generated by crustal melting

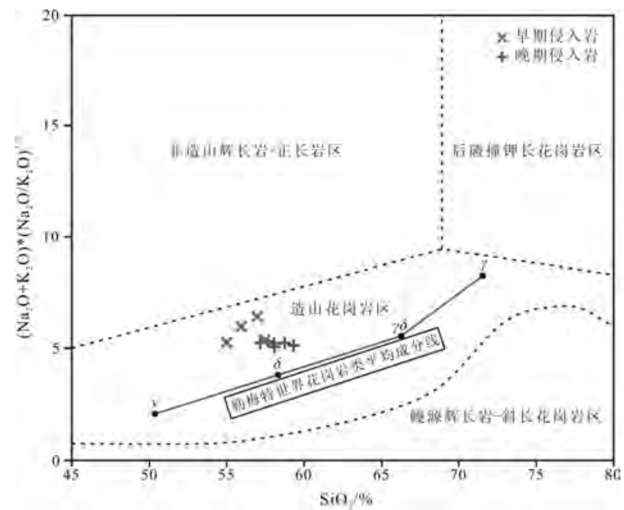

图5 帕什托克侵入岩序列SiO_2−(Na_2O+K_2O)*(Na_2O/K_2O)$^{1/2}$图
Fig.5 SiO_2−(Na_2O+K_2O)*(Na_2O/K_2O)$^{1/2}$ diagram of Pashtok intrusive sequence

随岩浆酸性增加而降低;而在过铝质岩浆中的磷灰石溶解度演化趋势相反,根据磷灰石此特征可进一步区分I型和S型[24−26]。帕什托克侵入序列属准铝质(图2−c),P_2O_5的含量很低,且随岩浆演化进一步降低(表1),具I型花岗岩演化趋势[27]。

4.2 构造环境分析

通过对岩浆岩地球化学数据分析,可以判断岩浆岩形成的大地构造环境或板块边界性质[30−34]。帕什托克侵入序列属造山花岗岩区中闪长岩,晚期侵入序列岩性愈加酸性(图5)。SiO_2−Y图(图6−a)、SiO_2−Yb图(图6−b)、SiO_2−Nb(图6−c)和SiO_2−Rb图(图6−d)反映帕什托克侵入序列可能为火山岛弧花岗岩或同碰撞花岗岩(VAG+Syn−COLG),且Y与Yb的含量在侵入序列演化过程中变化不明显,Rb有略微增加,Nb在演化过程中含量不稳定。Y−Nb图(图6−e)、Yb−Ta图(图6−f)、(Y+Nb)−Rb图(图6−g)、Yb+Ta−Rb图(图6−h)均指示帕什托克侵入序列属火山岛弧型花岗岩类(VAG),且晚期具有向同碰撞花岗岩类(Syn−COLG)演化的趋势,投点落入板内花岗岩(WPG)和同碰撞花岗岩(Syn−COLG)反映投点分布不均匀,具大陆弧花岗岩特征,可能是由于岩浆向酸性分异导致的。QAP构造环境判别图(图6−j)和R_1−R_2图(图6−i)综合反映帕什托克侵入序列为处于破坏性活动板块边缘的碰撞前大陆弧花岗岩类(CAG),并指示在岩浆分异结晶作用晚期大陆弧花岗岩(CAG)向大陆碰撞型花岗岩(CCG)演化,反映该类花岗岩与俯冲作用有关,且库地洋正处在大洋演化的衰退期。

选取典型火山岛弧型花岗岩(VAG)和碰撞花岗岩(COLG)与帕什托克侵入序列进行特征微量元素对比,反映帕什托克侵入序列的特征微量元素配分曲线与智利典型活动大陆边缘VAG曲线趋势类似(图7−a),但帕什托克侵入序列较富集高场强元素,且Y与Yb强富集,表明在岩浆结晶分异过程中可能存在Y与Yb分配系数大于1的矿物。对比Brown的三种构造环境花岗岩,该侵入序列与正常大陆弧花岗岩的曲线近似(图7−b),但强富集Rb、Th和Yb,反映岩浆向酸性演化,且结晶分异过程中存在Yb分配系数较大的石榴石控制Yb的富集[33−34],而Yb极强富集也表明可能存在壳源物质混染岩浆。与典型构造环境花岗岩对比,帕什托克侵入序列属活动大陆边缘I型科迪勒拉花岗岩(图7−c～d),与上述分析结果一致,并反映大陆弧构造环境复杂,除大陆弧存在俯冲外,还可能

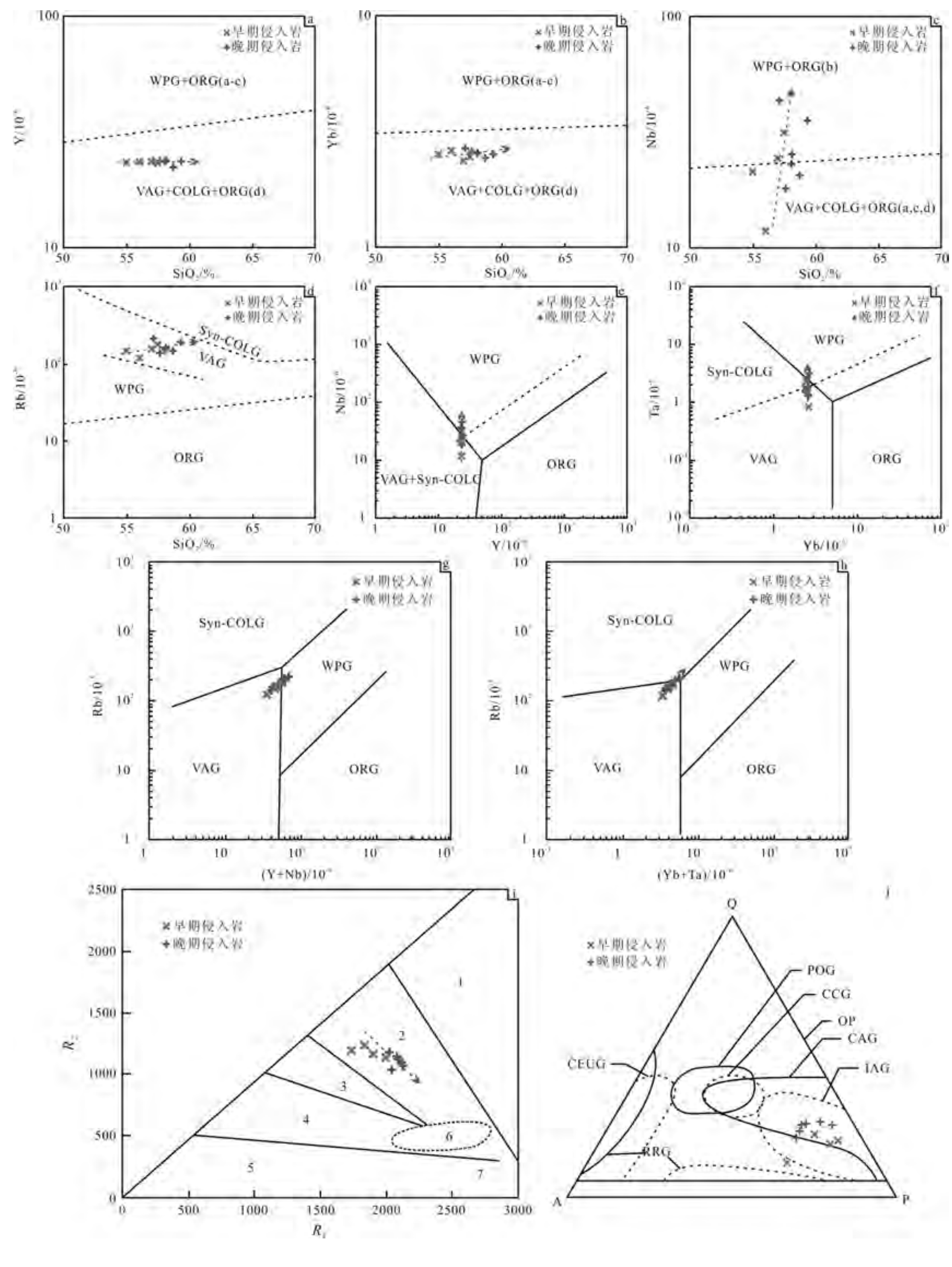

图6 帕什托克侵入序列构造判别图解

a—Y−SiO₂图；b—Yb−SiO₂图；c—Nb−SiO₂图；d—Rb−SiO₂图；e—Nb−Y图；f—Ta−Yb图；g—Rb−(Y+Nb)图；h—Rb−(Yb+Ta)图[35]；WPG—板内花岗岩；ORG—洋脊花岗岩；ORG(a)—正常洋脊花岗岩；ORG(b)—异常洋脊花岗岩；ORG(c)—弧后盆地洋脊花岗岩；ORG(d)—超俯冲洋脊花岗岩；VAG—火山岛弧花岗岩；COLG—碰撞花岗岩；Syn−COLG—同碰撞花岗岩；i—R_1−R_2图解；1—地幔斜长花岗岩；2—破坏性活动板块边缘(板块碰撞前)花岗岩；3—板块碰撞后隆起期花岗岩；4—晚造山期花岗岩；5—非造山期A型花岗岩；6—同碰撞(S型)花岗岩；7—造山期后A型花岗岩；j—QAP花岗岩构造环境判别图；CEUG—大陆造陆抬升花岗岩；RRG—与裂谷有关的花岗岩；POG—造山期后花岗岩；CCG—大陆碰撞带花岗岩；OP—大洋斜长花岗岩；CAG—大陆弧花岗岩；IAG—岛弧带花岗岩

Fig.6 Tectonic discrimination diagrams of Pashtok intrusive sequence.

a−Y−SiO_2 diagram; b−Yb−SiO_2 diagram; c−Nb−SiO_2 diagram; d−Rb−SiO_2 diagram; e−Nb−Y diagram; f−Ta−Yb diagram; g−Rb−(Y+Nb) diagram; h−Rb−(Yb+Ta) diagram[35]; WPG−Within plate granite; ORG−Oceanic ridge granite; ORG(a)−Normal oceanic ridge granite; ORG(b)−Anomalous oceanic ridge granite; ORG(c)−Oceanic ridge granite in back−arc basin; ORG(d)−Oceanic ridge granite in supra−subduction zone; VAG−Volcanic arc granite; COLG−Collision granite; Syn−COLG−Syn−collision granite; i−R_1−R_2 diagram, 1−Mantle plagiogranite; 2−pre−plate collision granite; 3−granite during uplifting after plate collision; 4−serorogenic granite, 5−non−orogenic A−type granite; 6−syn−collision granite; 7−Post−orogenic A−style granite; j−QAP tectonic diagram; CEUG−Continental epeirogenic uplift granitoids; RRG−Rift−related granitoids; POG−Post−orogenic granitoids; CCG−Continental collision granitoids; OP−Oceanic plagiogranites; CAG−Continental arc granitoids; IAG−Island arc granitoids

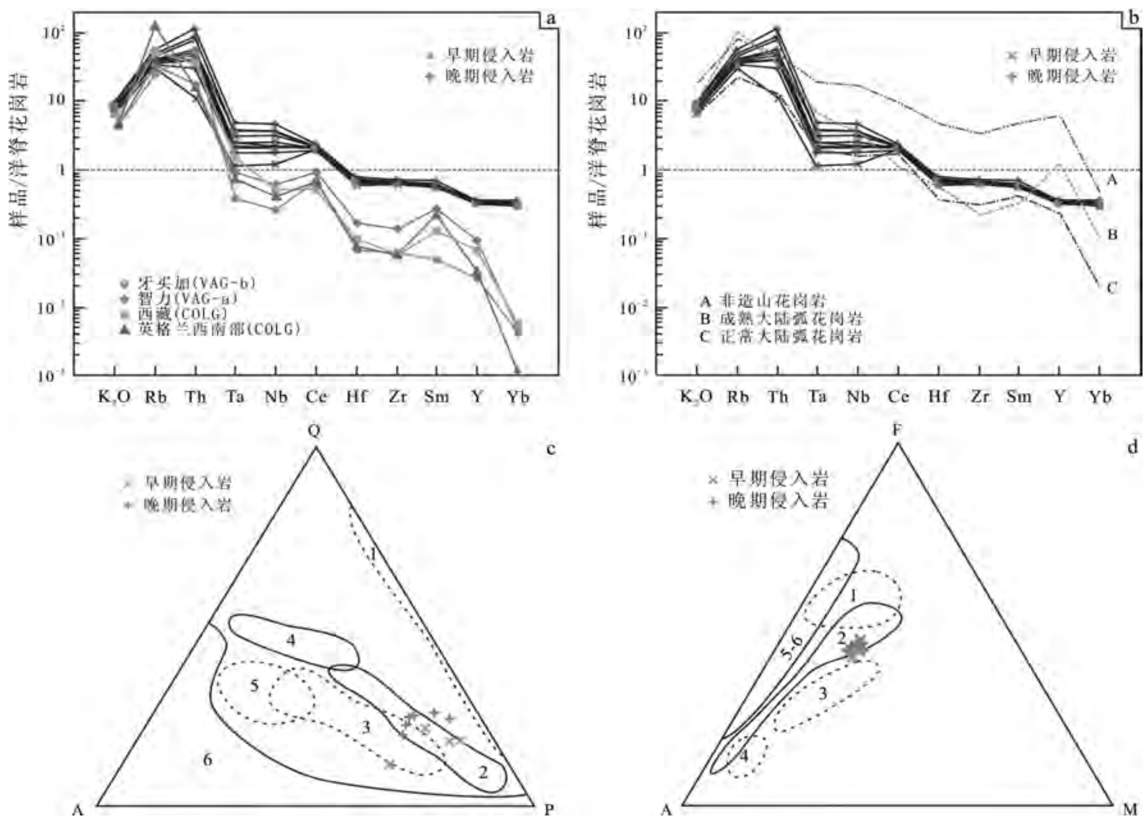

图7 微量元素配分曲线和构造环境判别图解

a，b—微量元素洋脊花岗岩标准化配分曲线；c—典型构造环境花岗岩QAP图解[36]；d—典型构造环境花岗岩AMF图解[36]；1—塞浦路斯、阿曼大洋斜长花岗岩（幔源）；2—I型科迪勒拉花岗岩（活动陆缘）；3—I型加里东花岗岩（碰撞隆起）；4—澳大利亚二云母堇青石S型花岗岩（壳源，同碰撞）；5—澳大利亚东南褶皱带造山后A型花岗岩；6—尼日利亚非造山带A型花岗岩

Fig.7 Trace element patterns and tectonic discrimination diagrams

a,b−ORG−normalized spider diagrams; c−QAP diagram of the granite of typical tectonic setting[36]; d−AMF diagram of the granite of typical tectonic setting[36]; 2−Cordillera granite (active continental margin); 3−I−type Caledonian granites (collision uplift); 4−Australian two−mica cordierite S−type granites (crust with collision); 5−post−orogenic A−type granites in the southeast Australian fold belt; 6−Nigeria non−orogenic A−type granite

存在弧-陆碰撞，且岩浆上升侵位过程中可能跨越不同地壳域。

4.3 地球动力学探讨

经上述分析，帕什托克侵入序列为壳幔混合源，且大面积闪长岩侵入可能与元古宙前壳幔物质深熔或重熔有关。C/MF−A/MF图解反映帕什托克侵入序列确实存在幔源物质部分熔融（图8）。在岩浆演化过程中，帕什托克侵入序列向富石英富钾长石贫钠长石的方向演化，岩浆愈加酸性，且该侵入序列向高钾系列过渡（图9−a）。演化过程中的物理

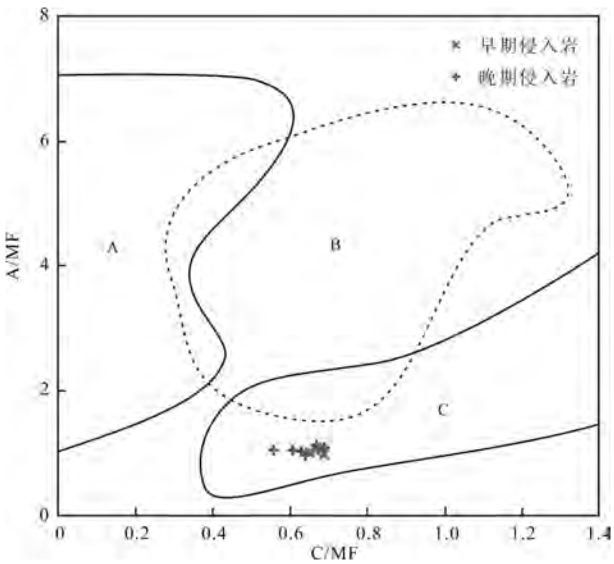

图8 C/MF−A/MF图解[38]
A—变质泥岩部分熔融;B—变质砂岩部分熔融;C—基性岩的部分熔融
Fig.8 C/MF−A/MF diagram of Pashtok intrusive sequence[38]
A−Partial melting of metamorphic mudstone; B−Partial melting of metamorphic sandstone; C−Partial melting of mafic rock

条件发生改变,侵入温压均下降,至演化晚期,该侵入序列集中在700 ℃、250 MPa的低温槽(图9−a;图9−b),反映该序列为深熔岩浆花岗岩,根据温压条件判断该侵入序列可能是幔源岩浆侵位下地壳和上地壳的产物[37]。

本文认为帕什托克侵入序列的形成与库地洋岩石圈俯冲有关,由于在俯冲背景下,库地洋在俯冲过程中诱导幔源岩浆上升侵位,提供使得元古宙前古老地壳物质重熔的充足热量,侵位幔源岩浆与重熔壳源物质混染后形成帕什托克侵入序列I型花岗岩母岩浆[40−66]。帕什托克侵入序列强富集Rb,平均含量为161.6×10^{-6},根据Condie研究Rb−Sr与地壳厚度关系[37],地壳厚度在30 km以上,随着岩浆向酸性演化,地壳厚度不断加厚(图10),反映该序列从活动陆缘花岗岩向同碰撞型花岗演化过程是板块汇聚俯冲、陆壳增厚的环境,且构造判别图解(图6)投点大部分都落于VAG中,说明该花岗岩与俯冲作用有关或者岩石的源区与俯冲作用直接相关。中元古代的岩浆事件在全球广泛分布[45−68],且主要记录了板块汇聚造山运动和哥伦比亚超级大陆的裂解与Rodinia超级大陆的聚合[45−68]。中元古代后期,塔里木古陆块和柴达木古陆块均发生了强烈的俯冲碰撞事件,完成了克拉通化,形成了华南统一基底,构成了Rodinia超级大陆的一部分[59−66],这与上述分析的构造背景一致,说明存在使得库地洋消亡的俯冲作用。

5 结论

(1)帕什托克侵入序列为花岗闪长岩系列,属准铝质高钾钙碱性岩类,该侵入序列分两期,早期侵入岩为石英闪长岩−石英二长闪长岩组合,晚期

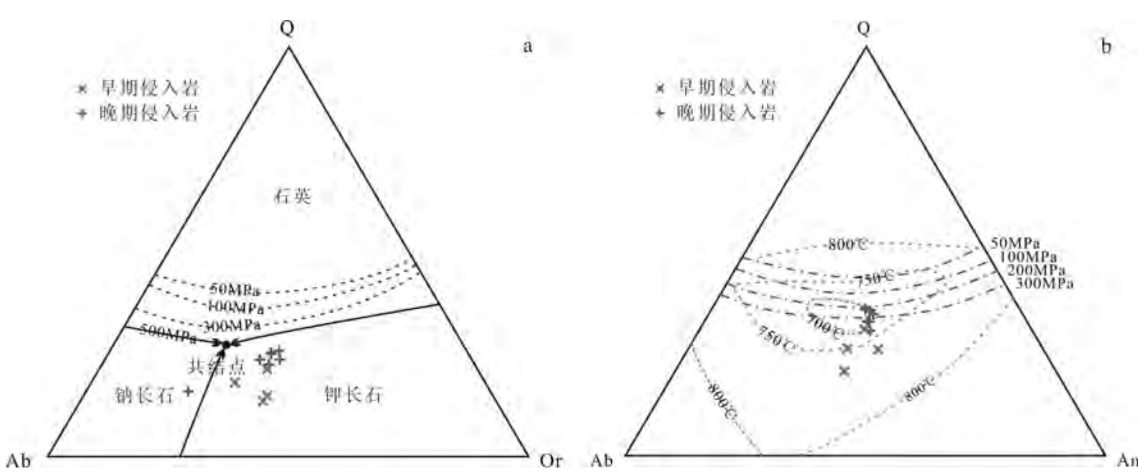

图9 帕什托克侵入序列成岩环境判别图
a—Q−Ab−Or图解;b—Q−Ab−An图解
Fig.9 Diagenetic environment discrimination diagrams of Pashtok intrusive sequence
a−Q−Ab−Or diagram; b−Q−Ab−An diagram

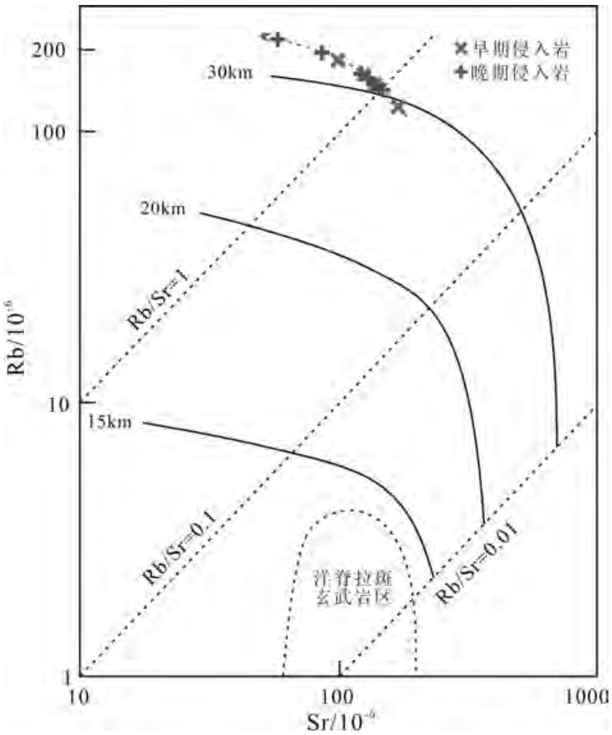

图10 Rb−Sr图解[39]

Fig.10 Rb−Sr diagram of Pashtok intrusive sequence[39]

侵入岩为英云闪长岩-花岗闪长岩组合。该侵入序列与I型花岗岩类似,其主量元素和微量元素均具典型I型花岗岩特征。

(2)帕什托克侵入序列为处于活动板块边缘碰撞前的大陆弧花岗岩类,两期侵入岩属同源岩浆演化,且由中性向酸性演化。形成帕什托克侵入序列的物源为壳幔混合源,幔源岩浆混染壳源物质形成母岩浆,且上升侵位至上、下地壳过渡带。

(3)帕什托克侵入序列的形成与库地洋壳俯冲有关,该序列从活动边缘的大陆弧花岗岩向同碰撞型花岗岩(Syn−COLG)演化,说明库地洋正处在衰退期,并反映塔里木古陆块和柴达木古陆块相互汇聚,正在形成Rodinia超大陆的一部分。

致谢:《中国地质》编辑部的各位审稿专家对本文提出了宝贵意见与建议,并耐心对文章中所出现的问题给予了解答,同时中国地质大学(北京)实验中心提供了帮助,在此一并表示感谢。

参考文献(References):

[1] 潘裕生. 青藏高原第五缝合带的发现与论证[J]. 地球物理学报, 1994, 37(2): 184−192.
Pan Yusheng. The discovery and demonstration of fifth suture zone in Qinghai−Tibet Plateau[J]. Chinese Journal of Geophysics, 1994, 37(2): 184−192 (in Chinese with English abstract).

[2] 张传林, 杨淳, 沈加林, 等. 西昆仑北缘新元古代片麻状花岗岩锆石SHRIMP年龄及其意义[J]. 地质论评, 2003, 3: 239−244.
Zhang Chuanlin, Yang Chun, Shen Jialin, et al. The zircon SHRIMP age of Late Proterozoic gneissic granite of West Kunlun and its significance[J]. Geological Review, 2003, 3: 239−244 (in Chinese with English abstract).

[3] 陆松年, 李怀坤, 相振群. 中国中元古代同位素地质年代学研究进展述评[J]. 中国地质, 2010, 37(4): 1002−1013.
Lu Songnian, Li Huaikun, Xiang Zhenqun. Advances in the study of Mesoproterozoic geochronology in China: A review[J]. Geology in China, 2010, 37(4): 1002−1013(in Chinese with English abstract).

[4] 黎敦朋, 赵越, 胡健民, 等. 西昆仑山奇台达坂花岗岩锆石TIMS U−Pb测年及热演化历史分析[J]. 中国地质, 2007, 34(6): 1013−1021.
Li Dunpeng, Zhao Yue, Hu Jianmin, et al. Zircon TIMS U−Pb dating of the Qitaidaban granite in the West Kunlun Mountains and its thermal evolution history[J]. Geology in China, 2007, 34(6): 1013−1021(in Chinese with English abstract).

[5] Zhang C L, Dong Y G, Zhao Y, et al. Geochemistry of Mesoproterozoic volcanics in West Kunlun: Evidence for the plate tectonic evolution[J]. Acta Geologica Sinica, 2003, 78: 532−542.

[6] 方锡廉, 汪玉珍. 西昆仑山加里东期花岗岩类浅识[J]. 新疆地质, 1990, 8(2): 153−158.
Fang Xilian, Wang Yuzhen. Review: Caledonian granitoids in West Kunlun[J]. Xinjiang Geology, 1990, 8(2): 153−158 (in Chinese with English abstract).

[7] 姜春发. 昆仑开合构造[M]. 北京: 地质出版社, 1993: 58−100.
Jiang Chunfa. Opening−closing Tectonics of Kunlun[M]. Beijing: Geological Publishing House, 1993: 58−100(in Chinese).

[8] 刘伟新, 丁道桂, 王道轩, 等. 西昆仑造山带花岗岩的地质特征及其构造意义[M]. 北京: 地质出版社, 1996.
Liu Weixin, Ding Daogui, Wang Daoxuan, et al. Geological Characteristics of Granite of the West Kunlun Orogenic Belt and Its Tectonic Significance[M]. Beijing: Geological Publishing House, 1996 (in Chinese).

[9] 卜文瑞, 王廷印, 马亚杰. 华北克拉通北缘西段中元古代花岗岩类的特征及其形成构造环境[J]. 岩石学报, 2001, 17(4): 609−616.
Bu Wenrui, Wang Tingyin, Ma Yajie. Characteristics of Mesoproterozoic granitoids of the western part of northern margin of the North China Craton and its tectonic environment[J]. Acta Petrologica Sinica, 2001, 17 (4): 609−616 (in Chinese with English abstract).

[10] 董永观, 郭坤一, 廖圣兵, 等. 新疆西昆仑科库西里克铅锌矿床地

质及元素地球化学特征[J]. 地质学报, 2007, 80(11): 1730−1738.
Dong Yongguan, Guo Kunyi, Liao Shengbing, et al. Geological and geochemical characteristics of lead−zinc deposit of the West Kunlun, Xinjiang[J]. Acta Geologica Sinica, 2007, 80(11): 1730 − 1738 (in Chinese with English abstract).

[11] 董永观, 郭坤一, 肖惠良, 等. 西昆仑地区成矿远景[J]. 中国地质, 2003, 30(2): 173−178.
Dong Yongguan, Guo Kunyi, Xiao Huiliang, et al. Mineralization prospective of West Kunlun[J]. Geology in China, 2003, 30(2): 173−178 (in Chinese with English abstract).

[12] 崔春龙, 范飞鹏, 李源, 等. 西昆仑北坡恰尔隆一带花岗岩类地球化学特征及构造背景初论[J]. 西南科技大学学报, 2009, 24(1): 48−55.
Cui Chunlong, Fan Feipeng, Li Yuan, et al. Geochemical characteristics of granitoid in the north slope of the West Kunlun and its tectonic setting[J]. Journal of Southwest University of Science and Technology, 2009, 24(1): 48− 55(in Chinese with English abstract).

[13] 巫建华, 刘帅. 大地构造学概论与中国大地构造学纲要[M]. 北京: 地质出版社, 2008.
Wu Jianhua, Liu shuai. Introduction to Geotectonics and Outline of Chinese Earth Tectonics[M]. Beijing: Geological Publishing House, 2008(in Chinese).

[14] 张传林, 陆松年, 于海锋, 等. 塔里木西南缘中元古代末期大陆汇聚及新元古代大陆裂解[C]//2004年全国岩石学与地球动力学研讨会论文摘要集. 2004.
Zhang Chuanlin, Lu Songnian, Yu Haifeng, et al. Proterozoic continental convergence and Neoproterozoic continental breakup in the southwest margin of Tarim[C]//The National Petrology and the Earth Dynamics Conference in 2004, 2004 (in Chinese with English abstract).

[15] 邱家骧, 林景仟. 岩石化学[M]. 北京: 地质出版社, 1991.
Qiu Jiaji, Lin Jingqian. Petrochemistry[M]. Beijing: Geological Publishing House, 1991 (in Chinese).

[16] 冯炳贵, 柴耀楚. 昆仑花岗岩类的主要特征[M]. 北京: 地质出版社, 1993, 58−100.
Feng Binggui, Chai Yaochu. The Main Features of Kunlun Granitoids[M]. Beijing: Geological Publishing House, 1993: 58−100 (in Chinese).

[17] Le Maitre, Bateman P, Dudek A, et al. A Classification of Igneous Rocks and Glossary of Terms: Recommendations of the International Union of Geological Sciences Subcommission on the Systematics of Igneous Rocks[M].Oxford Blackwell, 1989: 193.

[18] Barker F. Trondhjemite: Definition, environment and hypotheses of origin[J]. 1979: 1−12.

[19] Maniar P D, Piccoli P M. Tectonic discrimination of granitoids[J]. Geological Society of America Bulletin, 1989, 101(5): 635−643.

[20] Middlemost E A K. Magmas and magmatic rocks: An introduction to igneous petrology[J]. New York, 1985, 1(1): 266.

[21] Collins W J, Beams S D, White A J R, et al. Nature and origin of A− type granites with particular reference to southeastern Australia[J]. Contributions to Mineralogy and Petrology, 1982, 80 (2): 189−200.

[22] Chappell B W, White A J R. Two contrasting granite types[J]. Pacific Geology, 1974, 8(2): 173−174.

[23] 姜耀辉, 周珣若, 芮行健, 等. 西昆仑造山带花岗岩岩石系列及成因类型[J]. 地质学报, 2001, 75(1): 144−155.
Jiang Yaohui, Zhou Xunruo, Rui Xingjian, et al. Series and genesis type of granite of West Kunlun orogenic belt[J]. Acta Geologica Sinica, 2001, 75(1): 144−155(in Chinese with English abstract).

[24] 李献华, 李武显, 李正祥. 再论南岭燕山早期花岗岩的成因类型与构造意义[J]. 科学通报, 2007, 52(9): 981−991.
Li Xianhua, Li Wuxian, Li Zhengyang. Genesis type and tectonic significance of the early Yanshan granites in the Nanling[J]. Chinese Science Bulletin, 2007, 52(9): 981−991(in Chinese).

[25] 马鸿文. 西藏玉龙斑岩铜矿带花岗岩类与成矿[M]. 武汉: 中国地质大学出版社, 1990.
Ma Hongwen. Granite and Mineralization of Porphyry Copper Belt in Tibet[M]. Wuhan: China University of Geosciences Press, 1990(in Chinese).

[26] 杨克明. 论西昆仑大陆边缘构造演化及塔里木西南盆地类型[J]. 地质论评,1994, 1: 9−18.
Yang Keming. Tectonic evolution of continental margin on the West Kunlun and type of southwestern Tarim Basin[J]. Geological Review, 1994, 1: 9−18 (in Chinese with English abstract).

[27] Loiselle M C, Wones D R. Characteristics and Origin of Anorogenic Granites[C]//Geological Society of America Abstracts with Programs, 1979, 11(7): 468.

[28] Sun S S, McDonough W F. Chemical and isotopic systematics of oceanic basalts: Implications for mantle composition and processes[J]. Geological Society, London, Special Publications, 1989, 42(1): 313−345.

[29] Lameyre J, Bowden P. Plutonic rock types series: Discrimination of various granitoid series and related rocks[J]. Journal of Volcanology and Geothermal Research, 1982, 14(1): 169−186.

[30] Chappell B W. Aluminium saturation in I− type and S− type granites and the characterization of fractionated haplogranites[J]. Lithos, 1999, 46(3): 535−551.

[31] Wu Fuyuan, Jahn B, Wilde S A, et al. Highly fractionated I−type granites in NE China (I): Geochronology and petrogenesis[J]. Lithos, 2003, 66(3): 241−273.

[32] Li Xianhua, Li Zhengxiang, Li Wuxian, et al. Initiation of the

Indosinian orogeny in South China: Evidence for a Permian magmatic arc on Hainan island[J]. The Journal of Geology, 2006, 114(3): 341−353.

[33] 朱弟成, 莫宣学, 王立全, 等. 西藏冈底斯东部察隅高分异 I 型花岗岩的成因: 锆石 U−Pb 年代学、地球化学和 Sr−Nd−Hf 同位素约束[J]. 中国科学(D 辑), 2009, 39(7): 833−848.
Zhu Dicheng, Mo Xuanxue, Wang Liqun, et al. Petrogenesis of highly fractionated I−type granites in the Chayu area of eastern Gangdese, Tibet: Constraints from zircon U−Pb geochronology, geochemistry and Sr−Nd−Hf isotopes[J]. Science in China (D), 2009, 39(7): 833−848(in Chinese).

[34] Mueller D. Plate tectonics and crustal evolution[J]. Eos, Transactions American Geophysical Union, 1998, 79(18): 220.

[35] Pearce J A, Harris N B W, Tindle A G. Trace element discrimination diagrams for the tectonic interpretation of granitic rocks[J]. Journal of Petrology, 1984, 25(4): 956−983.

[36] Lameyre J, Bowden P. Plutonic rock types series: Discrimination of various granitoid series and related rocks[J]. Journal of Volcanology and Geothermal Research, 1982, 14(1): 169−186.

[37] Maniar P D, Piccoli P M. Tectonic discrimination of granitoids[J]. Geological Society of America Bulletin, 1989, 101(5): 635−643.

[38] De La Roche H, Leterrier J, Grandclaude P, et al. A classification of volcanic and plutonic rocks using R_1−R_2 diagram and major−element analyses: Its relationships with current nomenclature[J]. Chemical Geology, 1980, 29(1): 183−210.

[39] Condie K C, Hunter D R. Trace element geochemistry of Archean granitic rocks from the Barberton region, South Africa[J]. Earth and Planetary Science Letters, 1976, 29(2): 389−400.

[40] 吴泰然. 花岗岩及其形成的大地构造环境[J]. 北京大学学报: 自然科学版, 1995, 31(3): 358−365.
Wu Tairan. Granite and tectonic environment of its formation[J]. Acta Scientiarum Naturalium Universitatis Pekinensis, 1995, 31 (3): 358−365(in Chinese with English abstract).

[41] Barbarin B. A review of the relationships between granitoid types, their origins and their geodynamic environments[J]. Lithos, 1999, 46(3): 605−626.

[42] 张旗, 潘国强, 李承东, 等. 花岗岩构造环境问题: 关于花岗岩研究的思考之三[J]. 岩石学报, 2007, 23(11): 2683−2698.
Zhang Qi, Pan Guoqiang, Li Chengdong, et al. Granite tectonic environment problems: Reflections on third granite research[J]. Acta Petrologica Sinica, 2007, 23(11): 2683−2698 (in Chinese with English abstract).

[43] 张旗, 王焰, 李承东, 等. 花岗岩的 Sr−Yb 分类及其地质意义[J]. 岩石学报, 2006, 22(9): 2249−2269.
Zhang Qi, Wang Yan, Li Chengdong, et al. Granite classification on the basis of Sr and Yb contents and its implications[J]. Acta Petrologica Sinica, 2006, 22(9): 2249−2269(in Chinese with English abstract).

[44] Condie K C. Plate Tectonics[M]. Butterworth−Heinemann, 1997.

[45] Wickham S M, Li Z L. Granite for instructions tectonic setting[J]. Geological Science and Technology Information, 1989, 4: 20.

[46] 刘学锋, 肖安成. 塔里木盆地西南缘构造形变特征[J]. 江汉石油学院学报, 1996, 18(2): 19−24.
Liu Xuefeng, Xiao Ancheng. Structural deformation characteristics of southwestern margin in Tarim Basin[J]. Journal of Jianghan Petroleum Institute, 1996, 18(2): 19−24(in Chinese with English abstract).

[47] 伍致中, 刘东海. 塔里木盆地西南坳陷的形成演化[J]. 新疆石油地质, 1996, 17(3): 211−218.
Wu Zhizhong, Liu Donghai. The formation and evolution of Southwest Depression of Tarim Basin[J]. Xinjiang Petroleum Geology, 1996, 17(3): 211−218(in Chinese with English abstract).

[48] 杨克明. 论西昆仑大陆边缘构造演化及塔里木西南盆地类型[J]. 地质论评, 1994, 40(1): 9−18.
Yang Keming. The formation and evolution of the Western Kunlun continental margin[J]. Geological Review, 1994, 40(1): 9−18(in Chinese with English abstract).

[49] 姚卫江, 陈文利, 肖燕, 等. 塔里木盆地西南坳陷周边山前的典型构造模式建立[J]. 新疆地质, 2009, (S1): 47−55.
Yao Weijiang, Chen Wenli, Xiao Yan, et al. Establishment of typical structural models for piedmont areas surrounding southwestern Tarim Depression[J]. Xinjiang Geology, 2009, (S1): 47−55(in Chinese with English abstract).

[50] 曲国胜, 李亦纲, 李岩峰, 等. 塔里木盆地西南前陆构造分段及其成因[J]. 中国科学(D辑), 2005, 35(3): 193−202.
Qu Guosheng, Li Yigang, Li Yanfeng, et al. Foreland tectonic segmentation and geneses of the southwestern Tarim Basin[J]. Science in China (Ser. D), 2005, 35(3): 193−202(in Chinese).

[51] 曲国胜, 李亦纲, 张宁, 等. 塔里木西南缘(齐姆根弧)前陆构造及形成机理[J]. 地质论评, 2004, 50(6): 567−576.
Qu Guosheng, Li Yigang, Zhang Ning, et al. A study on the foreland structure of the Qimugen Arc in Southwest Tarim and its genetic mechanism[J]. Geological Review, 2004, 50(6): 567−576, 588(in Chinese with English abstract).

[52] 孙宝生, 刘增仁, 王招明. 塔里木西南喀什凹陷几个地质问题的新认识[J]. 新疆地质, 2003, 21(1): 78−84.
Sun Baosheng, Liu Zengren, Wang Zhaoming. New knowledge on geology of Kashi Depression in Southwest Tarim[J]. Xinjiang Geology, 2003, 21(1): 78−84 (in Chinese with English abstract).

[53] 王光杰, 滕吉文, 张中杰. 中国华南大陆及陆缘地带的大地构造基本格局[J]. 地球物理学进展, 2000, 15(3): 25−43.
Wang Guangjie, Teng Jiwen, Zhang Zhongjie. Tectonic basic pattern of South China and its continental margin[J]. Progress in Geophysics, 2000, 15(3): 25−43(in Chinese with English abstract).

[54] 鲁新便, 何发岐, 赵洪生. 塔里木盆地西南缘构造带的地球物理特征、构造及其演化[J]. 石油物探, 1997, 36(1): 43−52.

Lu Xinbian, He Faqi, Zhao Hongsheng. The geophysical feature, structure, and evolution of the tectonic belt in the southwest margin of the Tarim basin[J]. Geophysical Prospecting for Petroleum, 1997, 36(1): 43−52(in Chinese with English abstract).

[55] Nyman M W, Karlstrom K E, Kirby E, et al. Mesoproterozoic contractional orogeny in western North America: Evidence from ca. 1.4 Ga plutons[J]. Geology, 1994, 22(10): 901−904.

[56] Åhäll K I, Connelly J. Intermittent 1.53−1.13 Ga magmatism in western Baltica: Age constraints and correlations within a postulated supercontinent[J]. Precambrian Research, 1998, 92(1): 1−20.

[57] Frost C D, Frost B R, Chamberlain K R, et al. Petrogenesis of the 1.43 Ga Sherman batholith, SE Wyoming, USA: A reduced, rapakivi−type anorogenic granite[J]. Journal of Petrology, 1999, 40 (12): 1771−1802.

[58] Barnes M A, Anthony E Y, Williams I, et al. Architecture of a 1.38− 1.34 Ga granite− rhyolite complex as revealed by geochronology and isotopic and elemental geochemistry of subsurface samples from west Texas, USA[J]. Precambrian Research, 2002, 119(1): 9−43.

[59] Vigneresse J L. The specific case of the Mid−Proterozoic rapakivi granites and associated suite within the context of the Columbia supercontinent[J]. Precambrian Research, 2005, 137(1): 1−34.

[60] 郭坤一, 张传林, 王家鑫, 等. 西昆仑东段北缘花岗岩微量元素及同位素地球化学[J]. 吉林大学学报: 地球科学版, 2002, 32(2): 116−121.

Guo Kunyi, Zhang Chuanlin, Wang Jiaxin, et al. Trace elements and isotopic geochemistry of the high−K calc−alkaline granites in north margin of eastern part of West Kunlun[J]. Journal of Changchun University of Science and Technology, 2002, 32(2): 116−121 (in Chinese with English abstract).

[61] 郭坤一, 张传林, 赵宇, 等. 西昆仑造山带东段中新元古代洋内弧火山岩地球化学特征[J]. 中国地质, 2002, 29(2): 161−166.

Guo Kunyi, Zhang Chuanlin, Zhao Yu, et al. Geochemistry of Meso− and Neoproterozoic intra− oceanic arc volcanic rocks in the eastern segment of the western Kunlun orogenic belt[J]. Geology in China, 2002, 29(2): 161−166 (in Chinese with English abstract).

[62] 邓晋福, 刘翠, 冯艳芳, 等. 高镁安山岩/闪长岩类(HMA)和镁安山岩/闪长岩类(MA): 与洋俯冲作用相关的两类典型的火成岩类[J]. 中国地质, 2010, 37(4): 1112−1118.

Deng Jinfu, Liu Cui, Feng Yanfang, et al. High magnesian andesitic/dioritic rocks (HMA) and magnesian andesitic/dioritic rocks (MA): Two igneous rock types related to oceanic subduction[J]. Geology in China, 2010, 37(4): 1112− 1118 (in Chinese with English abstract).

[63] 厚刚福, 孙雄伟, 李昌, 等. 塔里木盆地西南部叶城凹陷下白垩统克孜勒苏群扇三角洲沉积特征及模式[J]. 中国地质, 2012, 39 (4): 947−953.

Gou Gangfu, Sun Xiongwei, Li Chang, et al. Depositional features of the fan delta from lower Cretaceous Kezilesu Group in Yecheng sag, southwestern Tarim Basin[J]. Geology in China, 2012, 39(4): 947−953 (in Chinese with English abstract).

[64] 王永, 李德贵, 肖序常, 等. 西昆仑山前晚新生代构造活动与青藏高原西北缘的隆升[J]. 中国地质, 2006, 33(1): 41−47.

Wang Yong, Li Degui, Xiao Xuchang. Late Cenozoic tectonic movement in the front of the West Kunlun Mountains and uplift of the northwestern margin of the Qinghai− Tibetan Plateau[J]. Geology in China, 2006, 33(1): 41− 47 (in Chinese with English abstract).

[65] 宗文明, 高林志, 丁孝忠, 等. 塔里木盆地西南缘南华纪冰碛岩特征与地层对比[J]. 中国地质, 2010, 37(4): 1183−1190.

Zong Wenming, Gao Linzhi, Ding Xiaozhong, et al. Characteristics of Nanhuan diamictite (tillite) and stratigraphic correlation in the southwestern margin of Tarim Basin[J]. Geology in China, 2010, 37(4): 1183− 1190(in Chinese with English abstract).

[66] 李涛, 王宗秀. 塔里木地块北部横向构造及断条模式[J]. 中国地质, 2006, 33(1): 14−27.

Li Tao, Wang Zongxiu. Transverse structure and model of fault slivers in the northern part of the Tarim block[J]. Geology in China, 2006, 33(1): 14−27 (in Chinese with English abstract).

Mesoproterozoic Pashtok diorite intrusive sequence on the northern margin of West Kunlun orogenic belt in Xinjiang and its geological implications

ZHAO Jia−nan[1, 2], LIU Zheng−jun[3]

(1. *School of Earth Sciences and Resources, China University of Geosciences, Beijing* 100083*, China;* 2. *State Key Laboratory for Continental Tectonics and Dynamics, Institute of Geology, Chinese Academy of Geological Sciences, Beijing* 100037*, China;* 3. *Hunan Institute of Geological Sciences, Changsha* 410007*, Hunan, China*)

Abstract: Pashtok intrusive sequence, located in the southwestern margin of the Tarim Block and the northern margin of the West Kunlun orogenic belt, is composed of quartz diorite and quartz monzonitic diorite, which is similar to TTG combination. It was formed in the late Mesoproterozoic. Large quantities of data prove that the strata and rocks located in the northern edge of West Kunlun orogenic belt still retain the records of orogenic events, plate subduction and convergence at the end of Mesoproterozoic, and they confirm that late Mesoproterozoic southwestern Tarim paleoplate belongs to the present active continental margin. Tarim ancient block was a part of Rodinia supercontinent. The early Paleozoic closure of the Kuda Ocean was closely related to the subduction between Kuda crust and Tarim ancient block. At the beginning of geochemical analysis, main elements and trace elements of Pashtok intrusive sequence were studied in detail. A discussion was made concerning the genesis of the intrusive sequence, the tectonic setting and the geodynamic model between plates around the intrusive sequence. The research shows that Pashtok intrusive sequence is of the I−type metaluminous high−K calc−alkaline granodiorite series, which belongs to continental arc granitoids of active continental margin. The intrusive sequence is divided into two intrusive periods. Both periods of intrusive rocks experienced comagmatic evolution, and the parental magma was a mixture of crustal materials and mantle magma, which gradually evolved into more acidic magma. Based on physical environment and tectonic setting in the course of magmatic evolution, the authors have reached the conclusion that the subduction of the Kuda Ocean crust brought about the closure of the Kuda Ocean and the convergence between Tarim ancient block and Qaidam ancient block which were pieced together and gradually became a part of the Rodinia supercontinent.

Key words: West Kunlun orogenic belt; Pashtok diorite intrusive sequence; geochemistry; tectonic setting; geodynamics

About the first author: ZHAO Jia−nan, male, born in 1989, doctor candidate, mainly engages in the study of oil and gas reservoir, the remote sensing geological prospecting, tectonics and structural geology; E−mail: zhaojianan1989@163.com.